The Structure-AChE Inhibitory Activity Relationships Study in a Series of Pyridazine Analogues

M. Saracoglu[1,*] and F. Kandemirli[2]

[1]*Faculty of Education, Erciyes University, 38039, Kayseri, Turkey;* [2]*Department of Chemistry, Kocaeli University, 41000, Izmit, Turkey*

Abstract: The structure-activity relationships (SAR) are investigated by means of the Electronic-Topological Method (ETM) followed by the Neural Networks application (ETM-NN) for a class of anti-cholinesterase inhibitors (AChE, 53 molecules) being pyridazine derivatives. AChE activities of the series were measured in IC_{50} units, and relative to the activity levels, the series was partitioned into classes of active and inactive compounds. Based on pharmacophores and antipharmacophores calculated by the ETM-software as sub-matrices containing important spatial and electronic characteristics, a system for the activity prognostication is developed. Input data for the ETM were taken as the results of conformational and quantum-mechanics calculations. To predict the activity, we used one of the most well known neural networks, namely, the feed-forward neural networks (FFNNs) trained with the back propagation algorithm. The supervised learning was performed using a variant of FFNN known as the Associative Neural Networks (ASNN). The result of the testing revealed that the high ETM's ability of predicting both activity and inactivity of potential AChE inhibitors. Analysis of HOMOs for the compounds containing *Ph1* and *APh1* has shown that atoms with the highest values of the atomic orbital coefficients are mainly those atoms that enter into the pharmacophores. Thus, the set of pharmacophores and antipharmacophores found as the result of this study forms a basis for a system of the anti-cholinesterase activity prediction.

Key Words: AChE, electronic-topological method, neural networks, pyridazine derivatives, structure-activity relationships.

INTRODUCTION

Alzheimer's disease (AD) associated with aging affects up to 5% of people over 65 years, rising to 20% of those over 80 years [1]. The disease is characterized by the presence of some neuropath logical markers detected in the brain of AD patients, which are the β-amyloid (βA) plaques and the neurofibrillary tangles. A pathogenic role is ascribed to these lesions, and many research programs that are focused on drugs capable of modifying the course of the disease are targeting both their formation and neurotoxicity [2].

One of a few undisputed evidences in the neuropathology of the AD is loss of cholinergic neurons occurring in different areas of the central nervous system (CNS), mainly the cerebral cortex and hippocampus, and it is not a surprise that the early pharmacological approaches to the treatment of the AD patients were aimed at increasing the availability of the cholinergic neuro-transmitter acetylcholine (ACh) [3]. On this basis, the cholinergic hypothesis became the leading strategy for the development of AD drugs [4, 5]. Tacrine was the first acetylcholinesterase (AChE) inhibitor launched in 1993 as the first drug for the symptomatic treatment of AD [6].

Three-dimensional quantitative structure–activity relationship (3D QSAR) studies were performed on AChE inhibitors, based on the molecular docking scores obtained by using FlexX and FlexiDock and comparative molecular field analysis (CoMFA) [7].

A diverse approach to the quantitative structure–activity relationship (QSAR) of tacrine derivatives against acetylcholinesterase (AChE) activity was applied in [8] using the variables selection for stepwise multiple linear regression (MLR), genetic algorithm (GA)-MLR, and simulated annealing (SA)-MLR. AChE activity (log RA) of tacrine derivatives was expressed with acceptable explanation (95.5–95.9%) and good predictive power (94.5–95.2%), respectively, in the models. The best equation was obtained from simulated annealing (SA) MLR with greater explanatory capability and better prediction, with a smaller standard error than other methods. The resulting models with the given descriptors illustrate the significant role of hydrophobic and electrostatic interactions for the AChE activity increase, while hydrophilic and topological features of molecules were shown to cause the decrease of AChE activity.

Quantitative structure–activity relationships (QSAR) studies on 24 *Amaryllidaceae* alkaloids being AChE inhibitors and belonging to five-membered ring systems, were carried out in [9] by using some physicochemical properties as their descriptors. Multiple linear regression analysis of the data has shown that strain energy, heat of formation and substituent's at both the aromatic ring and ring C play important roles in the development of the QSAR model. The contribution of substituent's at ring C to the model was further supported when strain energy was omitted from the model, and ring-type based QSAR analyses for the crinine- and lycorine-type alkaloids were performed. A number of CoMFA models

*Address correspondence to this author at the Faculty of Education, Erciyes University, 38039, Kayseri, Turkey; Tel: +90-352-4373206; Fax:+90-352-4378834; E-mail: muratsaracoglu@gmail.com

1573-4064/09 $55.00+.00

have already been developed on AChE inhibitors as well [10-13].

There are many methods for studying Structure-Activity Relationships (SAR), and all of them have some disadvantages. The purpose of the ETM [14-20] is to overcome the disadvantages of the molecular descriptions used in the previously developed SAR methods [12, 16].

ETM pays attention to both electronic and three-dimensional (3D) conformational structure of the compounds while previously developed QSAR methods mainly use just integral characteristics of the molecules. An integral characteristic, such as lipophilicity, solubility, dipole moment and molecular weight etc. represents a molecule as a whole. Thus, QSAR methods do not take into account details of molecular structure of the compounds under study arising from the electronic properties of separate atoms and bonds accessible through different programs for quantum-chemistry calculations and 3D topology optimization. The results of the ETM application can afterwards be used in quantitative calculations as well [21, 22].

Structure-AChE inhibitor activity relationship studies have been performed for three series of N-benzylpiperidine derivatives by means of the ETM application [18], which is a structural approach designed for the SAR investigation. Biological activities of the compounds belonging to three different series have been measured on mouse, human and *Torpedo californica* AChE. Molecular fragments that are only specific for active compounds ('activity features') were found for each series. In a similar way, "breaks of activity" (i.e. molecular fragments that are typical of inactive compounds and cannot be a part of an active compound) were calculated. Requirements necessary for a compound to be active were formulated as the result of detailed analysis of all compounds under study. The results obtained are in good agreement with common trends of ligand-receptor interactions detected by docking [23] and X-ray data analysis [24] of the N-benzylpiperidine derivatives.

Here, the SAR study for a class of electric eel AChE inhibitors related to pyridazine analogues was carried out by using the ETM. Their conformational and quantum-chemistry data were obtained by the molecular mechanics and semi-empirical quantum-chemistry methods. To develop the algorithmic base for the activity prediction, Artificial Neural Networks (ANN) was applied to the results of the ETM (the approach named as combined ETM-ANN method).

MATERIALS AND METHODS

Data Sets

The compounds under study are given in Table **1**, and their common skeletons are shown in the Scheme **1**.

Conformational analysis for a class of anti-cholinesterase inhibitors (AChE, 53 molecules) being pyridazine derivatives was performed by molecular mechanics. After this, the optimized structures were used in quantum-chemical calculations (AM1-method) [25] to obtain results providing input data for the ETM application. With the aim of more detailed SAR analysis, all compounds (53 in all) [26, 27] were separated into two classes according to their levels of activity; namely, active molecules with log $1/IC_{50} > 6.49$ (27 mol.) and inactive molecules with $IC_{50} \leq 6.49$ (26 mol.).

The ETM works with molecules represented by matrices, which are named electronic-topological matrices of conjunction (ETMC), because they are formed of electronic and 3D-topology data. Since details of the ETM can be found in literature [14-18], we give only the most distinguished properties of the ETM relative to other methods used in the SAR studies here.

Computations for the electronic-topological approach include the following steps [15-17]:

a. Conformational analysis.

b. Quantum-chemical calculations.

c. **ETMC** formation.

d. **ETMC** processing and search of the structural features of activity (pharmacophores-Ph) or inactivity (anti-pharmacophores-APh).

The main procedure of the **ETM** (implementing aforementioned phase's c, d) is described step by step below:

1. Provide descriptions (i.e. generate **ETMC**s) for all analyzed molecular structures.
2. Set initial parameters of the **ETM** algorithm.

The success of the ETM is determined by its specific compound structure description language (CSDL). Every compound is described by an $n \times n$ matrix (ETMC), where n is the number of atoms in the molecule. Conformational, quantum-chemical and physical-chemical data accompanying atoms and bonds of a molecule are used in the ETMCs. QSAR methods use some global chemical properties such as, lipophilicity, solubility, etc. Since each ETMC is symmetric with respect to its diagonal elements, only upper part of it is processed. Diagonal elements a_{ii}, where i mean the i-th atom in the molecule, represent one of the atomic parameters (such as atomic charge, valance activities, HOMO or LUMO energies, etc.). Off-diagonal elements a_{ij} can be of two kinds: one is for chemical bonds, and the other is for chemically non-bonded atoms. If i and j label chemically bonded atoms, then a_{ij} is a value characterizing one of the selected and fixed for all compounds electronic parameters of the i-j bond such as Wiberg's index, W_{ij} [28], bond energy (total, covalent or ionic), polarizabilty and so on. If i and j label non-bonded atoms, then a_{ij} is the interatomic distance between ith and jth atoms (R_{ij}). The ETMCs are easily understandable and extremely convenient for computer handling. In this way, the structures of the molecules under study get a unified description that is not bound to the atoms' identity. This circumstance is of primary importance for the search for pharmacophores in quite diverse structures of biologically active molecules.

Artificial Neural Networks (ANNs) represent a group of methods increasingly used in drug design for the QSAR studies [29, 30]. This method is especially capable of elucidating the structure-activity relationships when these relationships have a non-linear character. Thus, this method can be of significant interest for 3D QSAR studies.

Table 1. A List of Molecules Under Investigation

Compound	Skeleton Type	X	Y	Activity, Log 1/IC_{50}[a]	
				Exp.	Theo.
1	A		1	8.00	7.63
2	B	Me	H	7.68	7.69
3	A		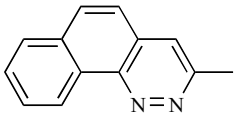	7.66	7.63
4	A		3	7.66	7.57
5	B	Et	H	7.57	7.56
6	A		2	7.41	7.51
7	C	3-Ac-Ph		7.27	7.47
8	C	3,5-$(CF_3)_2$-Ph		7.25	7.42
9	C	2-naphthyl		7.25	7.38
10	C	3-pyridinyl		7.24	7.37
11	C	3-AcNH-Ph		7.24	7.35
12	B	*i*-Pr	H	7.21	7.27
13	D	SCH_2CH_2	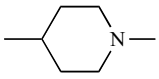	7.20	7.32
14	C	Cl		7.14	7.16
15	C	3,4-OCH_2O-Ph		7.14	7.14
16	C	2-Cl-Ph		7.10	7.11
17	C	2-Et-Ph		7.06	7.08
18	C	2-Me-Ph		7.05	7.04
19	C	2-thiophenyl		7.01	6.93
20	C	4-CN-Ph		7.00	6.96
21	C	2-MeO-Ph		6.96	6.84
22	B	H	H	6.92	6.92
23	E	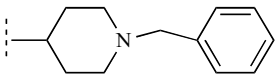	2	6.92	6.60
24	D	OCH_2CH_2	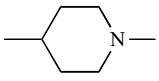	6.85	6.88
25	C	4-(NMe_2)-Ph		6.68	6.68
26	C	MeO		6.66	6.60
27	C	H		6.52	6.56
28	B	H	Me	6.49	6.49
29	C	4-F-Ph		6.46	6.43

(Table 1. Contd….)

Compound	Skeleton Type	X	Y	Activity, Log 1/IC_{50}[a]	
				Exp.	Theo.
30	B	H	*i*-Pr	6.37	6.38
31	B	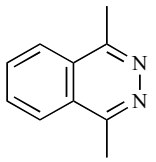		6.36	6.31
32	E	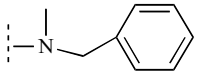	5	6.13	5.54
33	D	$NHCH_2CH_2$	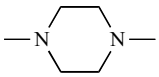	5.82	5.54
34	C	2,4,6-$(Me)_3$-Ph		5.52	5.71
35	D	$NHCOCH_2$		5.38	5.24
36	E	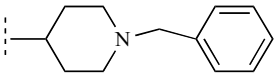	1	5.25	5.45
37	E	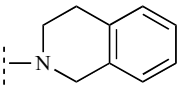	5	5.00	5.11
38	E	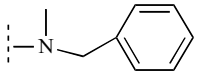	4	4.96	5.07
39	E	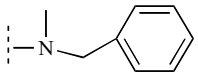	3	4.89	5.13
40		$NHCH_2CO$	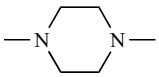	4.82	5.23
41	E	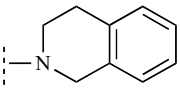	4	4.82	4.99
42	D	$NHCOCH_2$	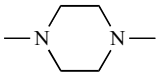	4.77	4.75
43	D	$NHCOCH_2$	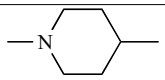	4.74	4.55
44	D	$NHCH_2CH_2$	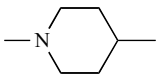	4.62	4.56
45	E	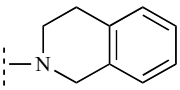	3	4.46	4.39
46	E	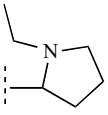	1	4.21	4.73

(Table 1. Contd….)

Compound	Skeleton Type	X	Y	Activity, Log 1/IC_{50}[a]	
				Exp.	Theo.
47	E	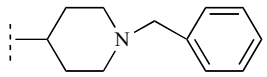	0	4.19	4.25
48	E	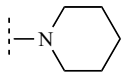	2	4.15	4.10
49	E	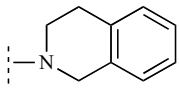	2	4.08	4.07
50	D	$NHCH_2CO$	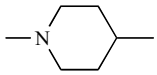	3.92	3.81
51	E	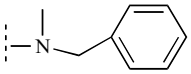	2	3.77	3.06
52	E	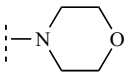	3	3.39	3.74
53	E	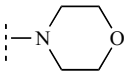	2	3.10	3.98

[a] IC_{50} in μM on electric eel AChE [26,27].

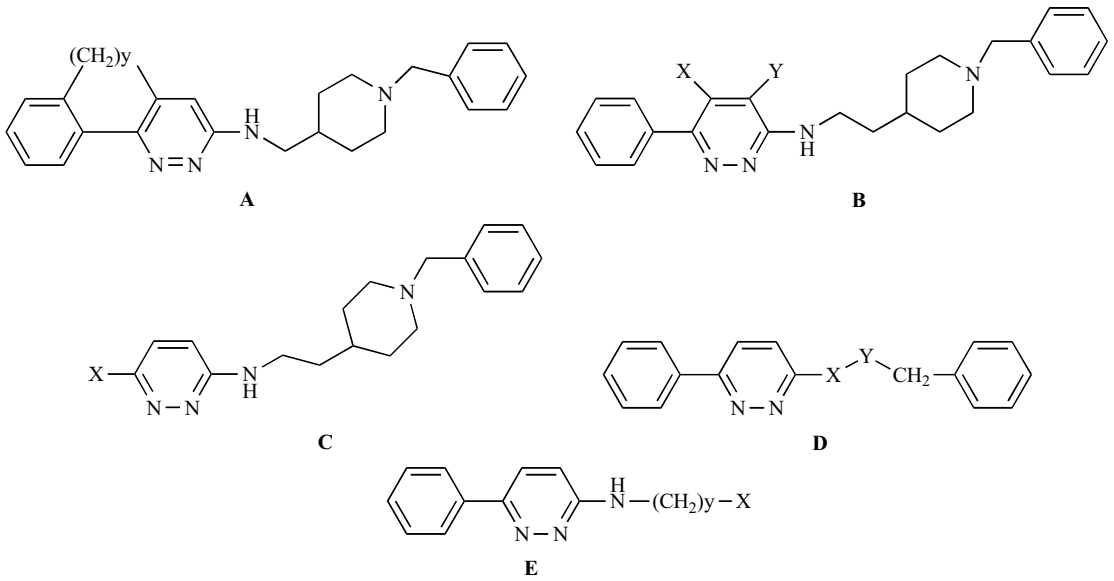

Scheme 1. Common molecular skeletons (**A-E**) of 3-[2-(1-benzylpiperidin-4-yl) ethylamino] pyridazine derivatives.

To have more stable activity features, *every* active molecule is used as a template for comparison with the rest of molecules. As a result of this comparison, activity features (pharmacophores) are revealed. To decide, which of the pharmacophores found is better, each inactive molecule is used as a template for comparison with the rest of molecules as well. So, inactivity features (anti-pharmacophores) also are a part of the system for the AChE inhibitory activity prediction.

RESULTS

The Search for Pharmacophores (Ph) and Anti-Pharmacophores (APh) by Using ETM

To apply ETM, data on the biological activity of compounds (qualified at least as being either active or inactive) and structures of the compounds are taken from outer databases or literature. (Ideally, half of the molecules should be active). Then the main steps of the ETM procedure are:

1. Conformational analysis. Minimize energy by using different optimization programs such as MMX (an extension of MM2 and MMP1), MMP2, and so on to get more reliable results depending on the complexity of the compounds [25, 31].

2. ETMCs formation. Matrices are formed of the data obtained from the quantum chemistry calculations for all molecular structures. The electronic structure of a compound may be determined by either of *ab initio* or semi empirical methods.

3. Initial settings. They are:

   – Some desirable level of probability (P_A) for the estimation of the frequency of an activity fragment occurrence in the analyzed molecules.

   – The threshold of activity needed to divide the series under study into classes of active and inactive molecules.

   – A template molecule that is to be compared with the rest of molecules in the series.

   – Some limiting values, δ_1 and δ_2, that are used to reflect the flexibility of the compounds; they allow for diagonal and off-diagonal values to be considered as equivalent ones in the limits defined by the user.

4. Search for structural fragments (through the comparison of all ETMCs with the template ETMC selected). The pharmacophores found only are to be common to all active molecules.

So, the aim of the core ETM's procedure is to find those fragments that, first, are common for all active compounds, and, second, satisfy some initial conditions (precision values and probability of their occurrence in active compounds). In the case, when either the estimation of the fragment by means of the probabilistic criterion P_A does not correspond to the level that has been set initially, or the fragments are not informative enough, template molecule and/or other initial settings are changed, and steps 3–5 are repeated. A common scheme of the ETM is shown in Fig. (**1**).

Under appropriate template molecule and other pre-set values, the activity features (or pharmacophores, Ph_i) can be used to predict the activity of interest for a new series of molecules with the help of the criteria P_A estimating each such feature. A criterion that is commonly used in structural methods for evaluating the probability of Ph_i occurrence in a series under study is given by the following formula:

$$P_A(Ph_i)=(n_A+1)/(n_A+n_{IA}+2),$$

where n_A, n_{IA} are numbers of active/inactive molecules, respectively, which contain the pharmacophore Ph_i. The same procedure can be done to determine features of inactivity, or 'breaks of activity', by choosing one of the inactive compounds as a template.

In accordance with the main steps of the ETM study, for all compounds in the series effective charges on atoms (Q_i, local atomic characteristics) were chosen as diagonal elements and either bond characteristics (Wiberg's indices, W_{ij}) or optimized distances (R_{ij}, in Å) were used as off-diagonal elements of their ETMCs.

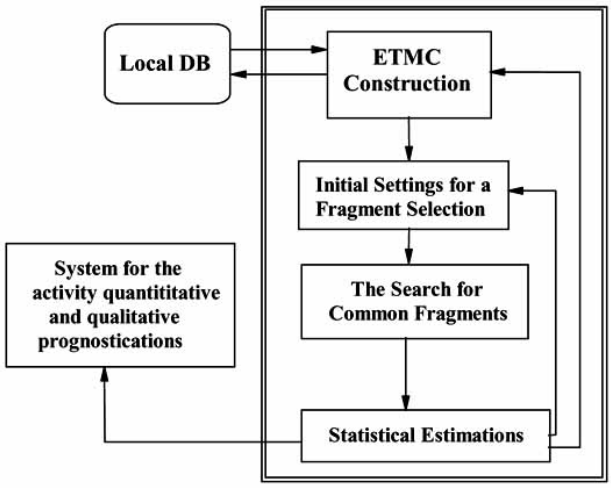

Fig. (1). The framework of the **ETM.**

For each molecule taken as a template, its ETMC was compared with the ETMCs of the rest of the molecules. The comparison resulted in a few common structural fragments being either pharmacophores or anti-pharmacophores. The fragments were found as sub matrices of the corresponding template ETMCs, high-active or low-active ones (their sub matrices are names ET-sub matrices of contiguity, or ETSCs, for short). A system for the activity prognostication was formed of the fragments of the two types, to predict 'activity' or 'inactivity' of an unknown compound.

DISCUSSION

Determination of Pharmacophores and Anti- Pharmacophores Features

The ETM-calculations detected *Ph1* pharmacophore found in 24 of 27 were high-active molecules. Thus, the probability P_A of its realization in this class is about 0.93. *Ph1*, its statistical estimate, and the corresponding ETSC ($ETSC_{Ph1}$) of the order 7x7, which has been calculated relative to the template compound **1**, are shown in Fig. (**2**). This sub-matrix was found after setting some allowable limits for the matrix elements comparison. For both classes, the limits for the diagonal and off-diagonal elements comparison are δ_1= 0.024 and δ_2= 0.06, respectively.

As seen from the pharmacophore structure, Ph1 consists of 7 atoms (C_{16}, C_{20}, C_{21}, N_{22}, C_{23}, C_{25} and C_{29}). The C_{20}-C_{21} pair of atoms, for example, is chemically bonded, and the bond order (Wiberg's index, W_{ij}) is 1.03 ē. The distance between N_{22} and C_{29} atoms (R_{ij}) is 4.44 Å.

Anti-pharmacophores (APh_i), along with pharmacophores, are also of interest for the researchers as those parts of molecules that are responsible for the considerable decrease or complete loss of the activity in view. To find anti-pharmacophores, inactive molecule 52 was selected as a template molecule. As an illustration, the *APh1* anti-

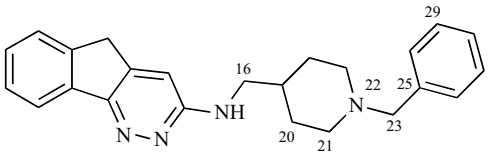

C_{16}	C_{20}	C_{21}	N_{22}	C_{23}	C_{25}	C_{29}
0.01	2.58	3.93	4.44	4.94	6.02	8.30
	0.01	1.03	2.52	3.09	4.50	6.80
		0.11	0.99	2.42	3.77	5.81
			-0.15	0.99	2.47	4.44
				0.10	1.02	3.86
δ_1= ±0.024, δ_2= ±0.06					0.02	2.46
n_A / n_{IA} =24/1, P_A= 0.93						0.01

Fig. (2). ETSC and corresponding structure of the pharmacophore *Ph1* found relative to active molecule **1**.

pharmacophore is shown in the Fig. (**3**), with corresponding sub-matrix given nearby.

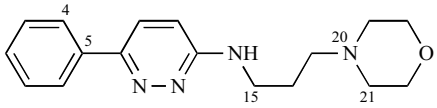

C_4	C_5	C_{15}	N_{20}	C_{21}
0.01	1.18	7.56	10.78	11.77
	0.03	6.46	9.85	10.73
		0.12	3.90	4.50
δ_1= ±0.04, δ_2= ±0.14			-0.15	0.99
n_{IA} / n_A=16/0, P_{IA} = 0.94				0.09

Fig. (3). ETSC and corresponding structure of the anti-pharmacophore *APh1* found relative to inactive molecule **52**.

The anti-pharmacophore *APh1* consists of 5 atoms enters the structures of 16 inactive molecules and is not found in active molecules (see Fig. (**3**)). The probability level of its realization is 94%. When comparing the structures of the pharmacophores and anti-pharmacophores, one can pay attention to the differences in their spatial and electron characteristics. Thus, pharmacophores and anti-pharmacophores can play their role in the activity prediction only if both types of fragments participate in the process of prognosis. Thus, the set of activity/inactivity fragments found as the result of this study forms a basis for a system of the anti-cholinesterase activity prediction. The statistic parameters of active and inactive compounds for studied series were given in Table **2**.

Table 2. Statistic Parameters of Active and Inactive Compounds for Studied Series

Predicted	Active	Inactive	Total
Pharmacophores	a=24	b=1	a+b=25
Antipharmacophores	c=0	d=16	c+d=16
Total	a+c=24	b+d=17	n=41

Sensitivity = a/(a+c) % of correctly= 24/24 = 100% predicted actives.

Specificity = d/(b+d) % of correctly= predicted inactives = 16/17 =94%.

Active Predictive Value = a/(a+b) % =24/25=96%predicted actives that are actually inactive.

Inactive Predictive Value = d/(c+d) = 16/16 = 100% predicted inactives that are actually active.

Concordance = (a+d)/n = 40/41 =98%.

The ability of the aforementioned system to divide compounds of the training set into classes of activity/inactivity is illustrated in Fig. (**4**) by the frequencies of the fragments occurrence in the compounds from the training set. The frequencies are shown in dependence with the level of anti-cholinesterase activity of the compounds in view.

As seen from the graph in the figure, in the class of active compounds, there is a group of high- active compounds and another group of compounds of low activity (named 'inactive compounds'). As seen from Fig. (**4**), the pharmacophores and anti-pharmacophores found as the result of the ETM application was used as a basis for a system formation that is capable of activity prediction for new derivatives.

The highest occupied molecular orbital's (HOMO) and the lowest unoccupied molecular orbital's (LUMO), called also *frontier orbital's* may also play an important role in the donor-acceptor interaction of a substance with the corresponding receptors. Analysis of HOMOs for the compounds containing *Ph1* and *APh1* has shown that atoms with the highest values of the atomic orbital coefficients are mainly those atoms that enter into the pharmacophores. Graphical representation of the HOMO orbitals is given in Fig. (**5**).

HOMO orbital for the template compound **1** consists of orbitals of those atoms that form piperidine and, partially, benzyl rings. In contrast to *Ph1*, HOMO orbital of *APh1* (compound **52**) consists of all atoms of morpholine ring and carbon atoms of propyl group. All the said suggests again an important role of these atoms in the substrate-receptor interaction.

Combined ETM-Artificial Neural Networks Approach (ETM-ANN)

The ETM data (initial matrices and the fragments found) were used in the NN applications with the aim of obtaining an algorithmic basis for the activity prediction (at place of manual processing). Here, some important observations related to their joint use are presented. To analyze the data, we used one of the most well known neural networks, namely, the feed-forward neural networks (FFNNs) trained with the back propagation algorithm [32, 33]. The supervised learning

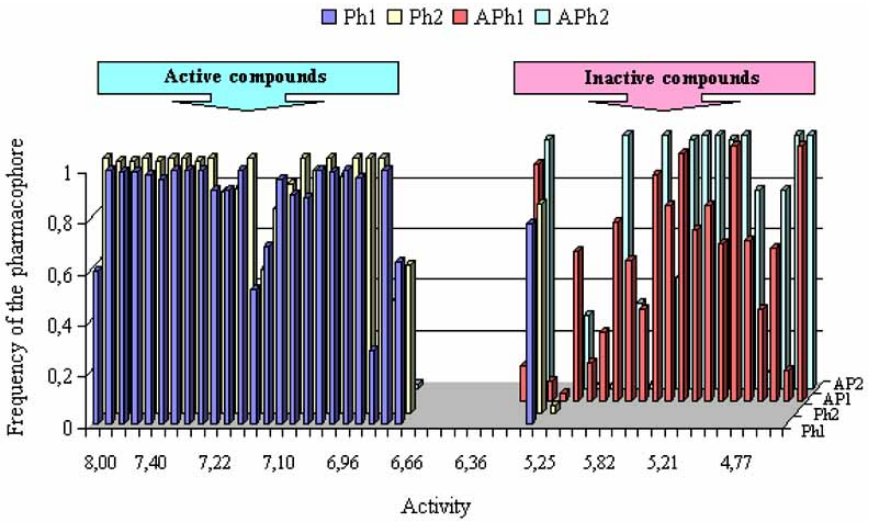

Fig. (4). Frequency of the fragments' occurrences in the compounds studied: for pharmacophores *Ph1* and *Ph2*; for anti-pharmacophores *APh1* and *APh2*.

was performed using a variant of FFNN known as the Associative Neural Networks (ASNN). Below, we briefly summarize the principles of this approach, while the detailed description of the algorithm can be found in literature [34]. The ASNN selected consists of three-layers with five neurons in one hidden layer. A single output node was used to code activities of the AChE inhibitors. The bias neurons were presented in the both input and hidden layers. At least M=100 independent FFNN were trained to analyze each set of variables. The predicted values of each analyzed case were averaged over all M network predictions and the means were used to calculate statistical coefficients with targets. The other details of the algorithm can be found elsewhere [35, 36].

The avoidance of over fitting/overtraining has been shown to be an important factor for improvement of predictive ability and correct selection of variables in the FFNNs. In short, the principal idea of the combined approach is to determine the weights of fragments represented by ETSCs and, afterwards, to use these *weights as descriptors* (WDs) for the ASNNs training. To do this, the fragments are being

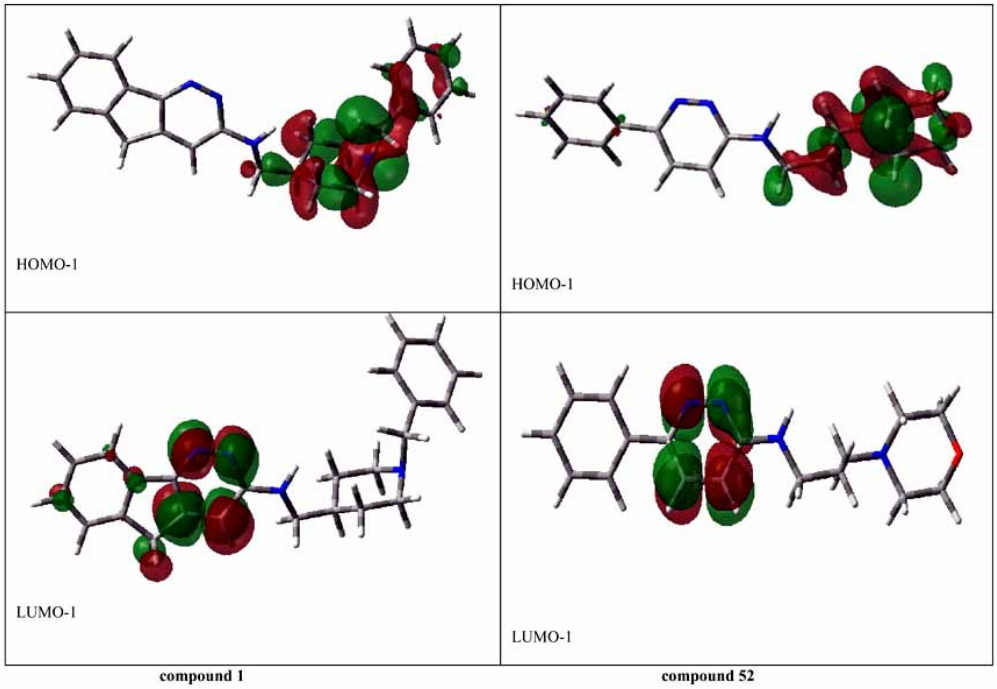

Fig. (5). A three-dimensional view of HOMO/LUMO orbitals for template compounds **1** and **52**.

projected on the Kohonen's maps that correspond to their initial ETMCs. In such way the degree of each fragment's presence in a molecule can be determined.

The first step is a procedure that can be called as "triples calculation". i.e. data elements in the initial set are triples *(d*1, *d*2, *d*3), where *d1* and *d2* are charges for a pair of atoms and *d3* is a connection between them. The values of *di*, *i*=1,2,3, are taken from the ETMCs. The total number of triples equals to the amount of all two-atomic connections taken from all ETMCs. Second step is the Kohonen's network (SOM) initialization and training (detailed description of a Kohonen's network can be found in [33]). The approximate number of elements in our Kohonen's map is calculated as $S=k*S_{ETM}$, where k varies in the range of [1.0, 2.0], and S_{ETM} is the size of the largest ETM matrix. The third step involves the calculations of pharmacophores as sub matrices of the template ETMCs. At the fourth step, the weight of each fragment (that is either a pharmacophore or antipharmacophore) is estimated versus each compound as the fragment's projection error, E_{ij}, relative to those nodes of the Kohonen's map that were found for its comprising ETMC. Then its weight is taken as the inverse of its error E_{ij}: $W_{ij}=1-E_{ij}/E_{max,j}$. Here i is the molecule's number, j is the fragment's number, and $E_{max,j}$ is the maximal error, for all j. A new table containing the calculated fragment weights (descriptors) is being formed for further ASNN training.

Briefly, the number of neurons in the input layer corresponds to the number of descriptors. The hidden layer contains five neurons. The bias neuron is presented both on the input and hidden layers. An ensemble of M=100 neural networks was trained. By this, the activity values of each compound were calculated for each ASNN and averaged over all M networks. This value was used to calculate cross-validation coefficients. The quality of the model was tested by the leave-one-out cross-validation q^2 value defined as

$$q^2 = (SD\text{-}press)/SD;$$

introduced by Cramer *et al*. [37]. Here *SD* represents the variance of a target value relative to its mean and *'press'* is the average squared errors of predicted values obtained from leave-one-out (LOO) procedure. By the method, each molecule is removed from the training set, and the remaining set is used to separate molecules into classes of activity, thereby predicting the activity of this molecule and evaluating the quality of the decision rule. The last step includes application of the pruning methods [38, 39] that aim in a set of the most relevant ETMC fragments selection.

These algorithms operate in a manner similar to step-wise multiple regression analysis and exclude at each step one input parameter that was estimated to be non-significant. The pruning algorithms were used in the current study to determine significant parameters of input data points of the analyzed molecules as described in references [38, 39].

To reflect the realistic internal structure of the data, all compounds were separated into two main classes, as it was said before. The first one included 27 active compounds, and the second series included 26 'inactive' compounds. For the data, 249 fragments were selected. The first step consisted of using the LOO cross-validation procedure for the total set of compounds. The ASNNs recognized correctly 92%, or 49 from 53 compounds. Next, the importance of the detected fragments for the observed activity was evaluated by using pruning methods. The most part of the fragments (taken as descriptors) were detected as non-significant and removed by the pruning algorithms. As the result, only 13 ETMC-fragments were chosen as the most important ones from 249 fragments in total. By this, ASNN classified correctly 94%, or 50 compounds from 53.

In Fig. (**6**), for template compounds 1 and 52 those molecular sides are shown where generalized ETSCs (one pharmacophore and one anti-pharmacophore) are realized. As seen from the figure, the atoms that enter the fragments found by means of ETM and ETM-NN are practically same.

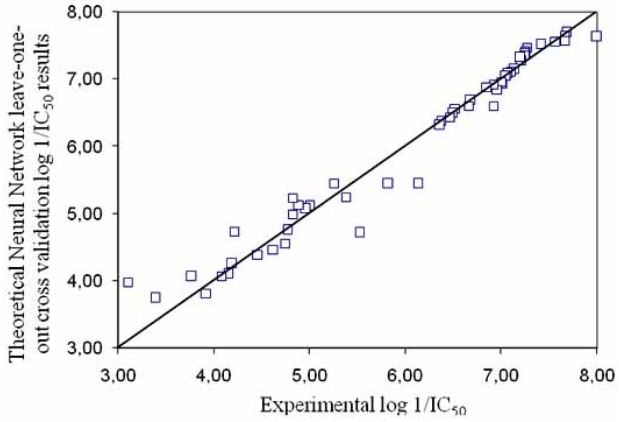

Fig. (6). Neural network leave-one-out cross-validation log $1/IC_{50}$ results.

The main goal of the second stage in the data analysis was to evaluate an efficacy of ASNN in the SAR model generation for the real values of the activity. The first step was the LOO cross-validation procedure applied to the total set of compounds. It has been found that a cross-validated q^2 coefficient of the ASNN predictions was 0.72±0.01. After applying the pruning methods but 9 fragments were selected from 249 in total, the cross-validated q^2 value was found as 0.88±0.01.

Thus, the obtained results indicate that application of pruning methods provides higher prognosing ability compared to the case when all descriptors are used for the activities prediction. As it is seen, the approach presented in this study has shown quite satisfactory results (Fig. (**7**)).

This fact tells in favor of workability of the both models found. These models can be applied to the design of new potent AChE inhibitory activity drugs.

CONCLUSION

A series of 3-[2-(1-Benzylpiperidin-4-yl) ethylamino] pyridazine anti-cholinesterase activity is studied by means of the ETM, which takes into account both structural and electronic characteristics of molecules. Based on pharmacophores and anti-pharmacophores calculated by the ETM-software as sub-matrices containing important spatial and quantum chemistry characteristics, a system for the activity prognostication is developed. The system was tested on a

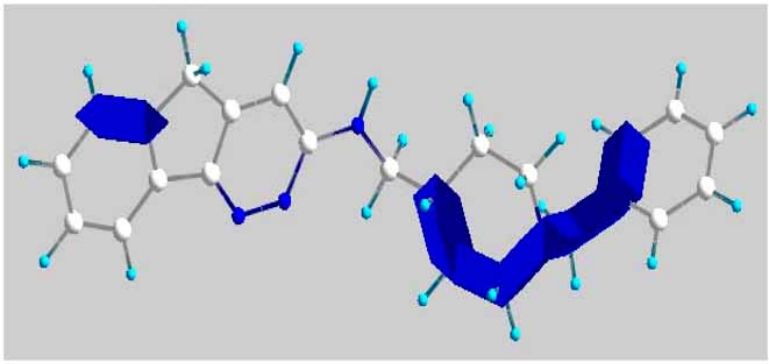

Compound **1.**

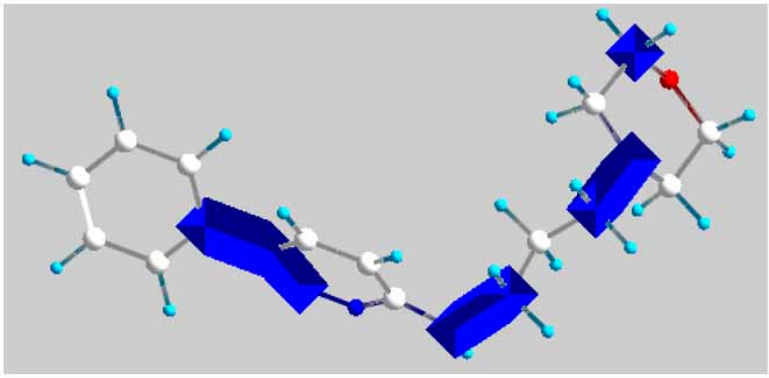

Compound **52.**

Fig. (7). Molecular fragments responsible for the AChE inhibitory activity's presence (compound **1**) and *'break of activity'* (compound **52**) found from the ETM-ASNN approach.

few molecules with molecular skeletons others than those that were characteristic of the training sets. It allows for identifying the presence/absence of the anti-cholinesterase activity (with probability of 93%) in molecules with diverse structures and predicting the level of the activity as well.

The initial data analysis witnesses the intimate relation of the activity exhibited by molecules to their spatial and electronic states. Any changes in the values of the matrices that excel the limits allowed cause diminishing or complete loss of the activity. The system for the anti-cholinesterase activity prediction is supposed to be used for the synthesis of new potent drugs. It makes screening and design of new potential drugs easy and effective.

ACKNOWLEDGEMENT

The authors would like to express their sincere gratitude to Prof. A. Dimoglo for the fruitful discussions of the results of this study and valuable help in preparing this manuscript to publishing.

REFERENCES

[1] Camps, P.; Achab, El R.; Morral, J.; Munoz-Torrero, D.; Badia, A.; Banos, J.E.; Vivas, N.M.; Barril, X.; Orozco, M.; Luque, F.J. New tacrine-huperzine a hybrids (huprines): highly potent tight-binding acetylcholinesterase ınhibitors of interest for the treatment of alzheimer's disease. *J. Med. Chem.*, **2000**, *43*, 4657-66.

[2] Rampa, A.; Piazzi, L.; Belluti, F.; Gobbi, S.; Bisi, A.; Bartolini, M.; Andrisano, V.; Cavrini, V.; Cavalli, A.; Recanatini, M.; Valenti, P. Acetylcholinesterase inhibitors: SAR and kinetic studies on omega-[N-methyl-N-(3-alkylcarbamoyloxyphenyl) methyl]aminoalkoxyaryl derivatives. *J. Med. Chem.*, **2001**, *44*, 3810-20.

[3] Davidsson, P.; Blennow, K.; Andreasen, N.; Eriksson, B.; Minthon, L.; Hesse, C. Differential increase in cerebrospinal fluid-acetylcholinesterase after treatment with acetylcholinesterase inhibitors in patients with alzheimer's disease. *Neurosci. Lett.*, **2001**, *300*, 157-60.

[4] Bartus, R.T.; Dean, R.; Beer, B.; Lippa, A. The cholinergic hypothesis of geriatric memory dysfunction. *Science*, **1982**, *217*, 408-14.

[5] Gualtieri, F.; Dei, S.; Manetti, D.; Romanelli, M.N.; Scapecchi, S.; Teodori, S. The medicinal chemistry of alzheimer's and alzheimer-like diseases with emphasis on the cholinergic hypothesis. *Il Farmaco*, **1995**, *50*, 489-503.

[6] Recanatini, M.; Cavalli, A.; Belluti, F.; Piazzi, L.; Rampa, A.; Bisi, A.; Gobbi, S.; Valenti, P.; Andrisano, V.; Bartolini, M.; Cavrini, V. SAR of 9-amino-1,2,3,4-tetrahydroacridine-based acetylcholinesterase inhibitors: synthesis, enzyme inhibitory activity, QSAR, and structure-based comfa of tacrine analogues. *J. Med. Chem.*, **2000**, *43*, 2007-18.

[7] Akula, N.; Lecanu, L.; Greeson, J.; Papadopoulos, V. 3D QSAR studies of AChE inhibitors based on molecular docking scores and CoMFA. *Bioorg. Med. Chem. Lett.*, **2006**, *16*, 6277-80.

[8] Jung, M.; Tak, J.; Lee, Y.; Jung, Y. Quantitative structure–activity relationship (QSAR) of tacrine derivatives against acetylcholinesterase (AChE) activity using variable selections. *Bioorg. Med. Chem. Lett.,* **2007**, *17*, 1082-90.

[9] Elgorashi, E.E.; Malan, S.F.; Stafford, G.I.; Staden, J. V. Quantitative structure–activity relationship studies on acetylcholinesterase enzyme inhibitory effects of Amaryllidaceae alkaloids. *South African J. Botany*, **2006**, *72*, 224-31.

[10] Hasegawa, K.; Kimura, T.; Funatsu, K. GA Strategy for variable selection in QSAR studies: application of GA-based region selection to a 3D-QSAR study of acetylcholinesterase inhibitors. *J. Chem. Inf. Comput. Sci.*, **1999**, *39*, 112-20.

[11] Bernard, P.; Kireev, D.B.; Chrétien, J.R.; Fortier, P.L.; Coppet, L. Automated docking of 82 N-benzylpiperidine derivatives to mouse acetylcholinesterase and comparative molecular field analysis with 'natural' alignment. *J. Comput.-Aided Mol. Des.*, **1999**, *13*, 355-71.

[12] Tong, W.; Collantes, E.R.; Chen, Y.; Welsh, W.J. A comparative molecular field analysis study of N-benzylpiperidines as acetylcholinesterase inhibitors. *J. Med. Chem.*, **1996**, *39*, 380-87.

[13] Cho, S.J.; Garsia, M.L;. Bier, J.; Tropsha, A. Structure-based alignment and comparative molecular field analysis of acetylcholinesterase inhibitors. *J. Med. Chem.*, **1996**, *39*, 5064-71.

[14] Dimoglo, A.S. Compositional approach to electronic structure description of chemical compounds, oriented computer analysis of structure-activity relation. *Khim.- Pharm.Zh.*, **1985**, *4*, 438-44.

[15] Shvets, N.M. Applied program system for the prognosis of biological activity of chemical compounds: development and use. *Comp. Sci. J. Moldova*, **1993**, *1*, 101-10.

[16] Shvets, N.M. The study of data and control flows and the user interface organization in an applied system used in chemistry and medicine for the biological activities prediction. *Comp. Sci. J. Moldova*, **1997**, *3*, 301-11.

[17] Dimoglo, A.S.; Vlad, P.F.; Shvets, N.M.; Coltsa, M.N. Structure–ambergris odour relationships investigation in a mixed series of decalin and non-decalin compounds: the electronic-topological approach. *New J. Chem.*, **2001**, *25*, 283-88.

[18] Dimoglo, A.S.; Shvets, N.M.; Tetko, I.V.; Livingstone, D.J. Electronic-topological investigation of the structure – acetylcholinesterase inhibitor activity relationship in the series of n-benzylpiperidine derivatives. *QSAR*, **2001**, *20*, 31-45.

[19] Dimoglo, A.S.; Gorbachov, M.Y.; Lesnik, T.I.; Saracoglu, M.; Güzel, Y.; Yildirim, I. Investigation of the relationship between chemical structure and anti-HIV-1 activity in a class of nucleoside analogues: electron-topological approach. *Curr. Med. Chem.*, **1997**, *4*, 23-34.

[20] Sim, E.; Dimoglo, A.; Shvets, N.M.; Ahsen, V. Electronic-topological study of the structure-activity relationships in a series of piperidine morphinomimetics. *Curr. Med. Chem.*, **2002**, *9*, 1537-45.

[21] Koçyiğit-Kaymakçıoğlu, B.; Oruç, E.; Unsalan, S.; Kandemirli, F.; Shvets, N.; Rollas, S.; Dimoglo, A. Synthesis and characterization of novel hydrazide–hydrazones and the study of their structure–antituberculosis activity. *Eur. J. Med. Chem.*, **2006**, *41*, 1253-61.

[22] Agirbas, H.; Guner, S.; Budak, F.; Keceli, S.; Kandemirli, F.; Shvets, N.; Dimoglo, A. Synthesis and structure–antibacterial activity relationship investigation of isomeric 2,3,5-substituted perhydropyrrolo[3,4-d]isoxazole-4,6-diones. *Bioorg. Med. Chem.*, **2007**, *15*, 2322-33.

[23] Bernard, P.; Kireev, D.B.; Chrétien, J.; Fortier, P.L.; Coppet, L. Automated docking of 82 n-benzylpiperidine derivatives to mouse acetylcholinesterase and comparative molecular field analysis with "natural" alignment. *J. Comput. Aided Mol. Des.*, **1999**, *13*, 355-71.

[24] Kryger, G.; Silman, I.; Sussman, J.L. Structure of acetylcholinesterase complexed with E2020 (Aricept®): implications for the design of new anti-Alzheimer drugs. *Structure*, **1999**, *7*, 297-07.

[25] Foresman, J.B.; Frisch, A. *Exploring Chemistry With Electronic Structure Methods*, 2th ed. Pittsburgh: PA, **1996**.

[26] Contreras, J.M.; Parrot, I.; Sippl, W.; Rival, Y.M.; Wermuth, C.G. Design, synthesis and structure–activity relationships of a series of 3-[2-(1-benzylpiperidin-4-yl)ethylamino]pyridazine derivatives as acetylcholinesterase inhibitors. *J. Med. Chem.*, **2001**, *44*, 2707-18.

[27] Contreras, J.M.; Rival, Y.M.; Chayer, S.; Bourguignon, J.J.; Wermuth, C.G. Aminopyridazines as acetylcholinesterase inhibitors. *J. Med. Chem.*, **1999**, *42*, 730-41.

[28] Wiberg, K.B. Application of the pople-santry-segal CNDO method to the cyclopropylcarbinyl and cyclobutyl cation and to bicyclobutane. *Tetrahedron*, **1968**, *24*, 1083-96.

[29] Kovesdi, I.; Dominguez-Rodrigue, M.F.; Orfi, L.; Naray-Szabo, G.; Varro, A.; Papp, J.G.; Matyus, P. Application of neural networks in structure-activity relationships. *Med. Res. Rev.*, **1999**, *19*, 249-69.

[30] Manallack, D.T.; Livingstone, D. J. Neural networks in drug discovery: have they lived up to their promise? *Eur. J. Med. Chem.*, **1999**, *34*, 195-08.

[31] Gilbert, K.; Gaevski, J. *A MMPMi Moleculer Mechanics Program*, Indiana University Bloomington: Indiana, **1985**.

[32] Rumelhart, D.E.; Hinton, G.E.; Williams, R.J. *Learning Internal Representations by Error Propagation. In Parallel Distributed Processing: Explorations in the Microstructure of Cognition*, The MIT Press; Cambridge, **1986**.

[33] Zupan, J., Gasteiger, J. *Neural Networks for Chemistry and Drug Design: An Introduction*, 2nd ed. VCH: Weinheim, **1999**.

[34] Dimoglo, A.; Kovalishyn, V.; Shvets, N.; Ahsen, V. The structure - inhibitory activity relationships study in a series of cyclooxygenase-2 inhibitors. A combined electronic-topological and neural networks approach. *Mini Rev. Med. Chem.*, **2005**, *5*, 879-92.

[35] Tetko, I.V.; Livingstone, D. J.; Luik, A. I. Neural network studies. 1: comparison of overfitting and overtraining. *J. Chem. Inf. Comput. Sci.*, **1995**, *35*, 826-33.

[36] Tetko, I.V.; Villa, A.E.P. Efficient partition of learning data sets for neural network training. *Neural Networks*, **1997**, *10*, 1361-74.

[37] Cramer, R.D.; Patterson, D.E.; Bruce, J.D. Comparative molecular field analysis (CoMFA): effect of shape on binding of steroids to carrier proteins. *J. Am. Chem. Soc.*, **1988**, *110*, 5959-67.

[38] Tetko, I.V.; Villa, A.E.P.; Livingstone, D.J. Neural network studies. 2. variable selection. *J. Chem. Inf. Comput. Sci.*, **1996**, *36*, 794-03.

[39] Kovalishyn, V.V.; Tetko, I.V.; Luik, A.I.; Kholodovych, V.V.; Villa, A.E.P.; Livingstone, D.J. Neural network studies. 3. variable selection in the cascade-correlation learning architecture. *J. Chem. Inf. Comput. Sci.*, **1998**, *38*, 651-59.

Received: 11 February, 2009 **Revised: 01 April, 2009** **Accepted: 02 April, 2009**